Supplementary Information

Solvent-dependent ultrafast deactivation processes with phenylpropyl indigo derivatives. A step forward in the understanding of indigo decay mechanisms

Daniela Pinheiro[a], Carla Cunha[a], Marta Pineiro[a], Adelino M. Galvão[b] and J. Sérgio Seixas de Melo*[a]

[a] University of Coimbra, CQC-ISM, Department of Chemistry, P3004-535 Coimbra, Portugal

[b] Universidade de Lisboa, Centro de Química Estrutural, Institute of Molecular Sciences, Av. Rovisco Pais, 1049-001 Lisboa, Portugal

Email: sseixas@ci.uc.pt (JSSM)

Table of Contents

EXPERIMENTAL SECTION

General procedures. Indigo (95%), sodium hydride (60% dispersion in mineral oil stored in a dry box) and 1-iodo-3-phenylpropane were obtained from commercial sources. All reagents used for the synthesis of the compounds were used without further purification. For the synthetic procedures, the solvents were of commercial pro analysis (P.A.) grade. For the spectral and photophysical determinations the solvents used were of spectroscopic or equivalent grade.

Steady-state UV-vis absorption/photoluminescence spectroscopy. Absorption and fluorescence spectra were recorded on a Carry 5000 UV-vis-NIR and Horiba Fluoromax 4 (or Fluorolog 3.22) spectrometers respectively. Fluorescence spectra were corrected for the wavelength response of the system.

Photoluminescence quantum yield. The fluorescence quantum yields (ϕ_F) at room temperature (T = 293 K) for **NPhC$_3$Ind** in the different solvents were obtained by the comparative method (Eq. 1) using indigo in DMF (ϕ_F = 0.0023)[1] as standard:

$$\phi_F^{cp} = \frac{\int I(\lambda)^{cp} d\lambda}{\int I(\lambda)^{ref} d\lambda} \cdot \frac{n_{cp}^2}{n_{ref}^2} \cdot \phi_F^{ref} \qquad (1)$$

where $\int I(\lambda)^{cp} d\lambda$ is the integrated area under the emission spectra of the compound (cp) solutions and $\int I(\lambda)^{ref} d\lambda$ of the reference (ref) solution, n_{cp}^2 and n_{ref}^2 are the refractive index of the solvents in which the compounds and the reference were respectively dissolved and ϕ_F^{ref} is the fluorescence quantum yield of the standard. The fluorescence quantum yields (ϕ_F) at T = 293 K for **N,N'PhC$_3$Ind** in the different solvents were obtained by the comparative method (Eq. 1) using the fluorescence quantum yields (ϕ_F) of **NPhC$_3$Ind** in the different solvents as standards.

Fluorescence quantum yields at T = 77 K were obtained by comparison with the spectrum at T = 293 K run under the same experimental conditions using Eq. 2,

$$\phi_F^{77\,K} = \frac{\int I(\lambda)^{77\,K} d\lambda}{\int I(\lambda)^{293\,K} d\lambda} \cdot \phi_F^{293\,K} \cdot f_c \qquad (2)$$

where $\int I(\lambda)^{x\,K} d\lambda$ is the integrated area under the emission of the compound at 77 K and 293 K, $\phi_F^{293\,K}$ is the fluorescence quantum yield at 293 K and f_c is the factor that considers the "shrinkage" of the solvent (volume) upon cooling, given by V_{77K}/V_{293K} (for 2-methyltetrahydofuran and methylcyclohexane is assumed f_c=0.8).[2]

Quantum electronic calculations All theoretical calculations were of the density functional theory (DFT) type, carried out using GAMESS-US version R3.[3] A range corrected LC-BPBE (ω=0.2 au^{-1}) functional, as implemented in GAMESS-US[3], was used in both ground- and excited-state

calculations. Time-dependent functional theory (TDDFT) calculations, with similar functionals, were used to probe the excited-state potential energy surface (PES). Solvent was included using the polarizable continuum model with the solvation model density to add corrections for cavitation, dispersion, and solvent structure. In the TDDFT calculation of Franck-Condon (FC) excitations the dielectric constant of the solvent was split into a "bulk" component and a fast component, which is essentially the square of the refractive index. In "adiabatic" conditions only the static dielectric constant was used. In DFT or TDDFT calculations a 6-31G** basis set was used.[3] The results obtained with the LC-BPBE(20) functional are essentially unscaled raw data from calculations; for the $S_0 \rightarrow S_n$ transitions, a small correction, which result in the subtraction of 0.05 eV, to account for the difference between zero point and the first vibronic level, was considered. For the resulting optimized geometries time dependent DFT calculations (using the same functional and basis set as those in the previously calculations) were performed to predict the vertical electronic excitation energies. Molecular orbital contours were plotted using ChemCraft 1.7 program. Frequency analysis for each compound were also computed and did not yield any imaginary frequencies, indicating that the structure of each molecule corresponds to at least a local minimum on the potential energy surface.

Time-resolved photoluminescence spectroscopy. Fluorescence decays were measured using a home-built picosecond time-correlated single photon counting (ps-TCSPC) apparatus described elsewhere.[4] The excitation source consists of a tunable picosecond Spectra-Physics mode-lock Tsunami laser (Ti:sapphire) model 3950 (80 MHz repetition rate, tuning range 700–1000 nm), pumped by a 532 nm continuous wave Spectra-Physics Millennia Pro-10s laser. The excitation wavelength (λ_{exc} = 433 nm) was obtained with a Spectra-Physics harmonic generator, model GWU-23PS. To eliminate stray light from the light source, an RG530 filter was placed between the sample holder and the emission monochromator. The fluorescence decay curves were deconvoluted using the experimental instrument response function signal collected with a scattering solution (aqueous Ludox solution). The deconvolution procedure was performed using the modulation function method, as implemented by G. Striker in the SAND program, and previously reported in the literature.[5]

Femtosecond transient absorption spectroscopy. The experimental setup for the ultrafast spectroscopic and kinetics measurements consisted of a broadband (350–1600 nm) HELIOS pump–probe femtosecond transient absorption spectrometer from Ultrafast Systems, pumped by an amplified femtosecond Spectra-Physics Solstice-100F laser (800 nm central wavelength, 128 fs pulse width and 1 kHz repetition rate) and coupled with a Spectra-Physics TOPAS Prime F optical parametric amplifier (195–22 000 nm tuning range). The probe light in the UV range was generated by passing a small portion of the 800 nm light from the Solstice-100F laser through a computerized optical delay (with a time window of up to 8 ns) and then focusing it on a vertical translating CaF2 crystal to generate a white-light continuum (350–750 nm). All the measurements were obtained in a 2 mm quartz cuvette, with absorptions of ~0.3 at the pump excitation wavelength. To avoid photodegradation, the solutions were stirred during the experiments or kept in movement with a frequency lower than that of the laser using a motorized translating sample holder. Background signals from impurities or unwanted coherent effects were ruled out by scans of the neat solvent. The spectral chirp of the data was corrected using

the Surface Xplorer PRO program from Ultrafast Systems. Global analysis of the data (using a sequential model) was performed using Glotaran software.[6]

Microwave (MW)-assisted reactions. Microwave (MW)-assisted reactions were performed in a CEM Discover S-Class single-mode microwave reactor, featuring continuous temperature, pressure and microwave power monitoring.

Analytical thin-layer chromatography (TLC). Analytical thin-layer chromatography (TLC) was performed on Macherey-Nagel ALUGRAM Xtra silica gel plates with UV254 indicator. Visualization was accomplished by using an ultraviolet lamp. Silica gel column was carried out with silica gel (230-400 mesh).

Nuclear magnetic resonance. Nuclear magnetic resonance (NMR) spectra were recorded at room temperature in deuterated chloroform ($CDCl_3$) solutions on a Bruker Avance III spectrometer and a Bruker DRX-400 spectrometer, both operating at 400.13 MHz for ^{1}H and 100.61 MHz for ^{13}C, and is given in Figure S1-4. Chemical shifts for ^{1}H and ^{13}C are expressed in ppm, relatively to an internal standard of TMS (tetramethylsilane). Chemical shifts (δ) and coupling constants (J) are indicated in ppm and Hz, respectively.

Gas chromatography-mass spectroscopy (GC-MS). Gas chromatography-mass spectroscopy (GC-MS) analyses was performed on a Hewlett-Packard 5973 MSD spectrometer, using electron ionization (EI) (70 eV), coupled with a Hewlett-Packard Agilent 6890 chromatography system, equipped with a HP-5 MS column (30 m $\times$ 0.25 mm $\times$ 0.25 µm) and high-purity helium as carrier gas. The initial temperature of 70 °C was increased to 250 °C at a 15 °C min^{-1} rate, and held for 10 min. Then the temperature was increased to 290 °C at a 5 °C min^{-1} rate and held for 2 min, giving a total run time of 32 min. The flow of the carrier gas was maintained at 1.33 mL min^{-1}. The injector port was set at 250 °C, and is given in Figure S5.

High-resolution mass spectrometry (HRMS). High-resolution mass spectrometry (HRMS) was performed on a Bruker microTOF-Focus mass spectrometer equipped with an electrospray ionization time-of-flight (ESI-TOF) source, and is given in Figure S6.

Synthesis of N-phenylpropylindigo and N,N'-diphenylpropylindigo Derivatives. In a thick-glass microwave reactor, with a magnetic stirring bar, indigo (200 mg, 1 equiv.) and sodium hydride (NaH) (2 equiv.) were dissolved in 1 mL N-dimethylformamide (DMF). Then 1-iodo-3-phenylpropane was added (4 equiv.) and solvent was added to a total volume of 2 mL. The resulting mixture was heated under microwave irradiation at 25 °C for 15 minutes. After cooling down to room temperature, the reaction mixture was extracted with dichloromethane and water and the organic layer was dried overnight with anhydrous sodium sulfate. After this, the mixture was filtered and the solvent concentrated under reduce pressure. The crude was purified by column chromatography (SiO_2) using ethyl acetate: hexane (1:3¸v/v) as an eluent to afford **NPhC$_3$Ind** as a blue solid (138 mg, 48% yield) and **N,N'PhC$_3$Ind** as a green solid (140 mg, 37% yield).

N-phenylpropylindigo (NPhC$_3$Ind): ^{1}H NMR ($CDCl_3$, 400 MHz), δ 10.80 (s, 1H), 7.71 (d, J=7.2 Hz, 1H), 7.68 (d, J=8.3 Hz, 1H), 7.48 (dd, J=1.2 Hz, J=7.2 Hz, 1H), 7.45 (dd, J=1.1 Hz, J=7.1 Hz, 1H), 7.25 –7.18 (m, 5H), 6.99 (d, J=7.7 Hz, 2H), 6.97-6.92 (m, 1H), 6.88 (d, J=8.3 Hz, 1H), 4.54 (t, J=7.6 Hz, 2H), 2.71 (t, J=7.6 Hz, 2H), 2.07-2.00 (m, 2H) ppm. ^{13}C NMR ($CDCl_3$, 101 MHz), δ 189.9, 187.3, 152.5, 151.5, 141.4, 136.1, 135.9, 128.5, 128.5, 128.5, 128.51, 126.1, 125.6, 124.9, 124.3, 122.7, 120.8, 120.7, 120.6, 120.4, 111.9, 110.6, 46.6, 32.9, 29.9 ppm. GC-MS: m/z [M^+] = 380.2

N,N'-diphenylpropylindigo (N,N'PhCH$_3$Ind): ^{1}H NMR ($CDCl_3$, 400 MHz), δ 7.70 (d, J= 7.1 Hz, 2H), 7.47 (dt, J=1.2 Hz, J=7.2 Hz, 2H), 7.19-7.10 (m, 6H), 7.02 (t, J= 6.9 Hz, 6H), 6.96 (d, J= 8.2 Hz, 2H), 4.24 (t, J=7.6 Hz, 4H), 2.53 (t, J= 7.6 Hz, 4H), 1.93 (qui, J= 7.6 Hz, 4H) ppm. ^{13}C NMR ($CDCl_3$, 101 MHz), δ 185.6, 152.3, 140.8, 134.9, 128.4, 128.2, 126.1, 125.6, 124.2, 122.0, 121.2, 111.3, 47.3, 33.1, 28.7 ppm. HRMS (ESI-TOF-MS): m/z [M+H]$^+$ = 499.2380 calculated for $C_{34}H_{31}N_2O_2$; found: 499.2384

Table S1. Orbital contours of the HOMO and LUMO of indigo (IND), **NPhC$_3$Ind** and **N,N'PhC$_3$Ind** in DMF.

Compound	HOMO	LUMO
IND[a]	-6.89	-1.52
NPhC$_3$Ind	-6.73	-1.55
N,N'PhC$_3$Ind	-6.77	-1.58

[a]For indigo in DMF data from ref.[7]

Table S2. Absorption and emission maximum experimental (Exp.) and theoretical (Calc.) values, in different solvents, for **NPhC$_3$Ind**. The oscillator force (*f*) and the respective electronic transition (Trans.) are reported together with the data obtained at the level theory of the DFT//LC-BPBE(ω=0.2)

	Solvent	Exp. (Absorption)	Calc. (*f*)	Trans.
Absorption	**MCH**	629	621 (0.288)	H $\rightarrow$ L
	THF	633	621 (0.289)	
	DMF	640	624 (0.293)	
	DMSO	646	621 (0.297)	
Emission	**MCH**	659	663 (0.260)	H $\rightarrow$ L
	THF	673	694 (0.338)	
	DMF	692	707 (0.367)	
	DMSO	705	713 (0.364)	

Table S3. Photophysics of **NPhC$_3$Ind** by TDDFT in MCH and DMSO. The oscillator force (*f*) and the respective electronic transition are reported together with the data obtained at the level theory of the DFT//LC-BPBE(ω=0.2).

		TA (transient absorption)		
Solvent	**Form**	**nm**	***f***	S_1 to S_n
MCH	**Keto**	882	0.003	$S_1 \rightarrow S_4$
		642	0.306	$S_1 \rightarrow S_5$
		608	0.006	$S_1 \rightarrow S_6$
		552	0.049	$S_1 \rightarrow S_7$
	Dimer	802	0.000	$S_1 \rightarrow S_{10}$
		648	0.269	$S_1 \rightarrow S_{11}$
		641	0.011	$S_1 \rightarrow S_{12}$
		611	0.007	$S_1 \rightarrow S_{13}$
		562	0.011	$S_1 \rightarrow S_{14}$
DMSO	**Keto**	804	0.001	$S_1 \rightarrow S_4$
		609	0.313	$S_1 \rightarrow S_5$
		599	0.013	$S_1 \rightarrow S_6$
		514	0.112	$S_1 \rightarrow S_7$
	Dimer	785	0.000	$S_1 \rightarrow S_{10}$
		632	0.300	$S_1 \rightarrow S_{11}$
		619	0.017	$S_1 \rightarrow S_{12}$
		599	0.001	$S_1 \rightarrow S_{13}$
		550	0.012	$S_1 \rightarrow S_{14}$

Table S4. Absorption and emission maximum experimental (Exp.) and theoretical (Calc.) values, in different solvents, for **N,N'PhC$_3$Ind** (obtained of the conformer C_{OUT}). The oscillator force (*f*) and the respective electronic transition (Trans.) are reported together with the data obtained at the level theory of the DFT//LC-BPBE(ω=0.2).

	Solvent	**Exp. (Absorption)**	**Calc. (*f*)**	**Trans.**
Absorption	**MCH**	645	620 (0.242)	H → L
	THF	654	644 (0.231)	
	DMF	666	647 (0.235)	
	DMSO	673	647 (0.233)	
Emission	**MCH**	697	696 (0.236)	H → L
	THF	715	717 (0.316)	
	DMF	737	735 (0.347)	
	DMSO	750	758 (0.349)	

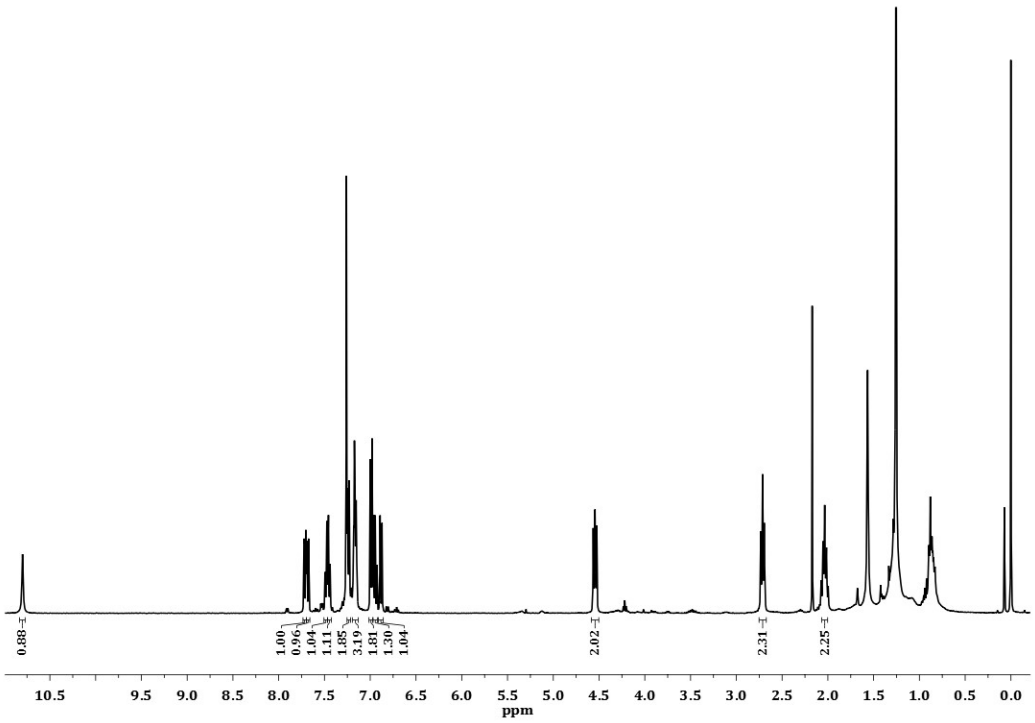

Figure S1. ^{1}H NMR of **NPhC$_3$Ind** in $CDCl_3$.

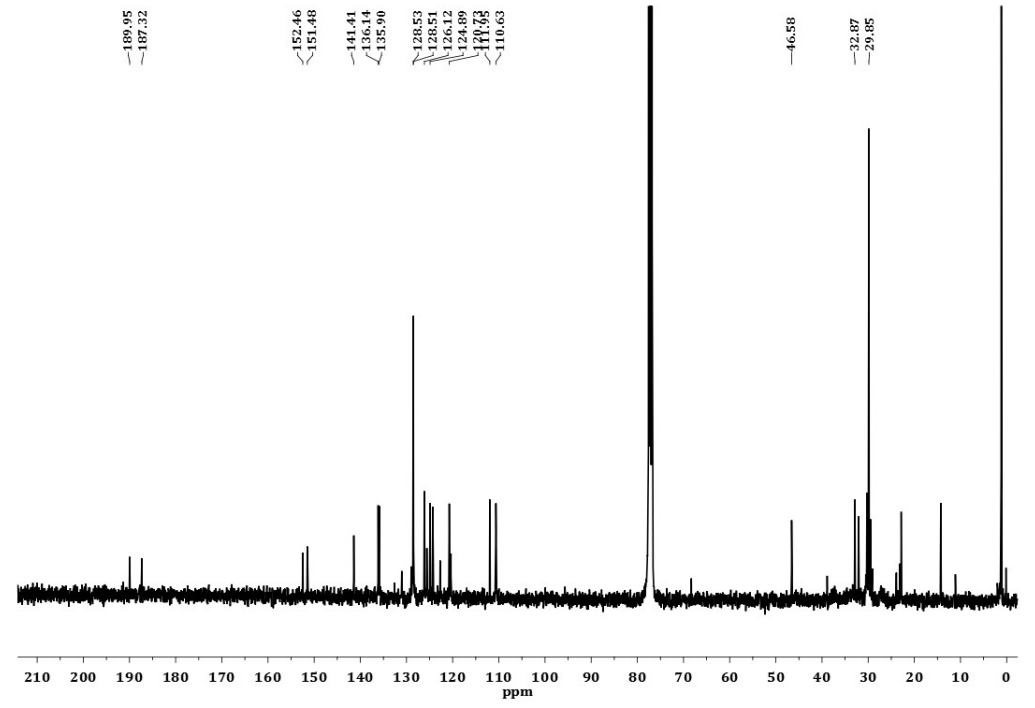

Figure S2. ^{13}C NMR of **NPhC$_3$Ind** in $CDCl_3$.

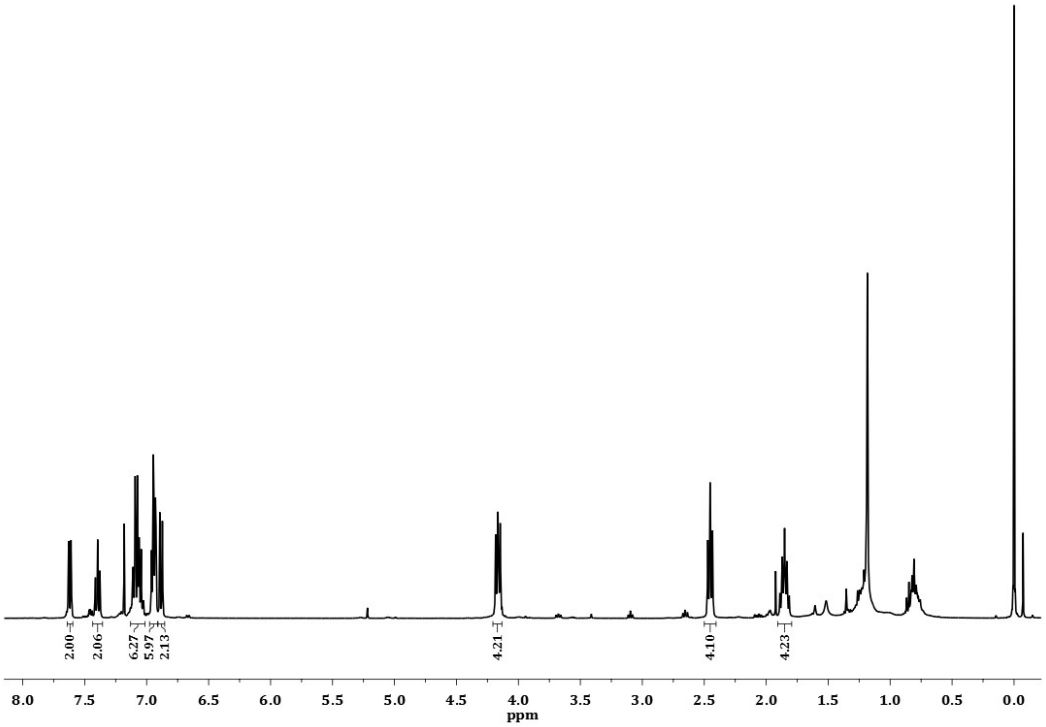

Figure S3. ^{1}H NMR of **N,N'PhC$_3$Ind** in $CDCl_3$.

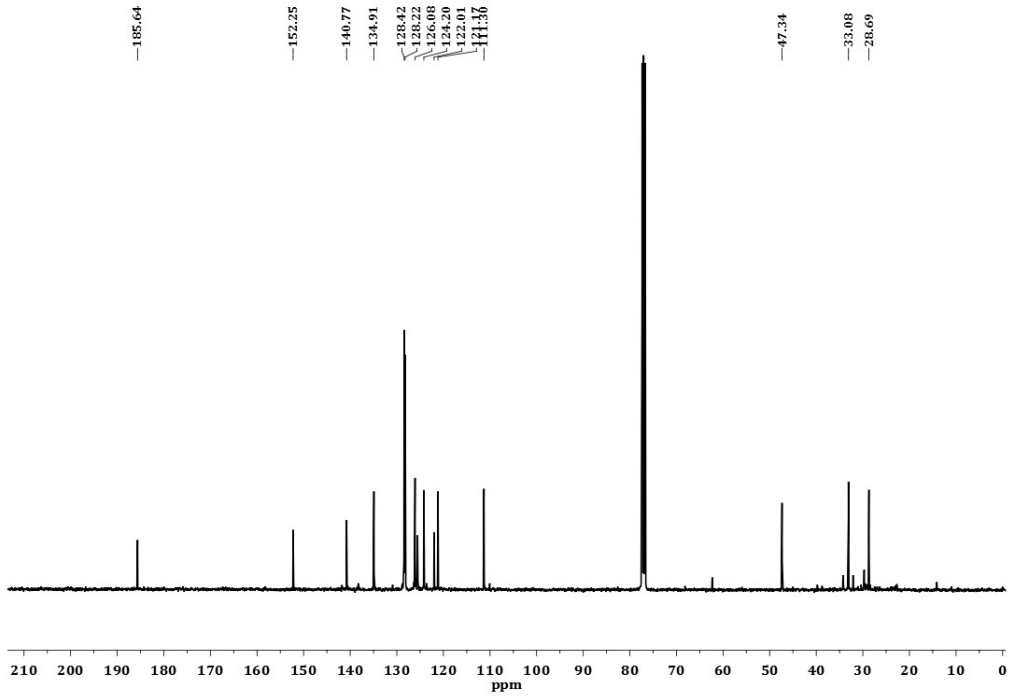

Figure S4. ^{13}C NMR of **N,N'PhC$_3$Ind** in $CDCl_3$.

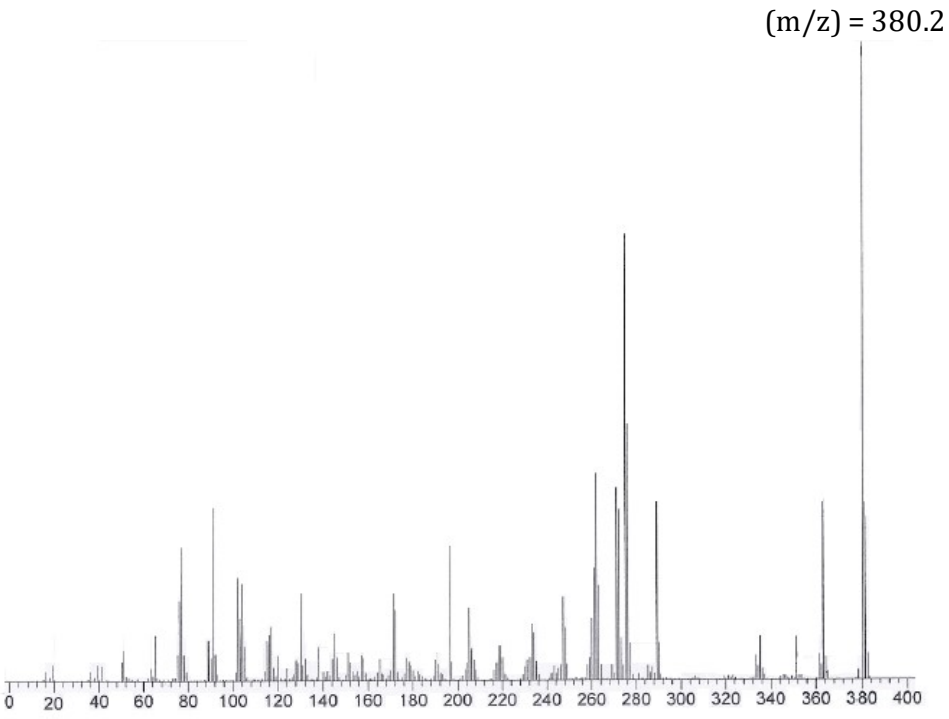

Figure S5. Gas chromatogram and mass spectra of **NPhC$_3$Ind**.

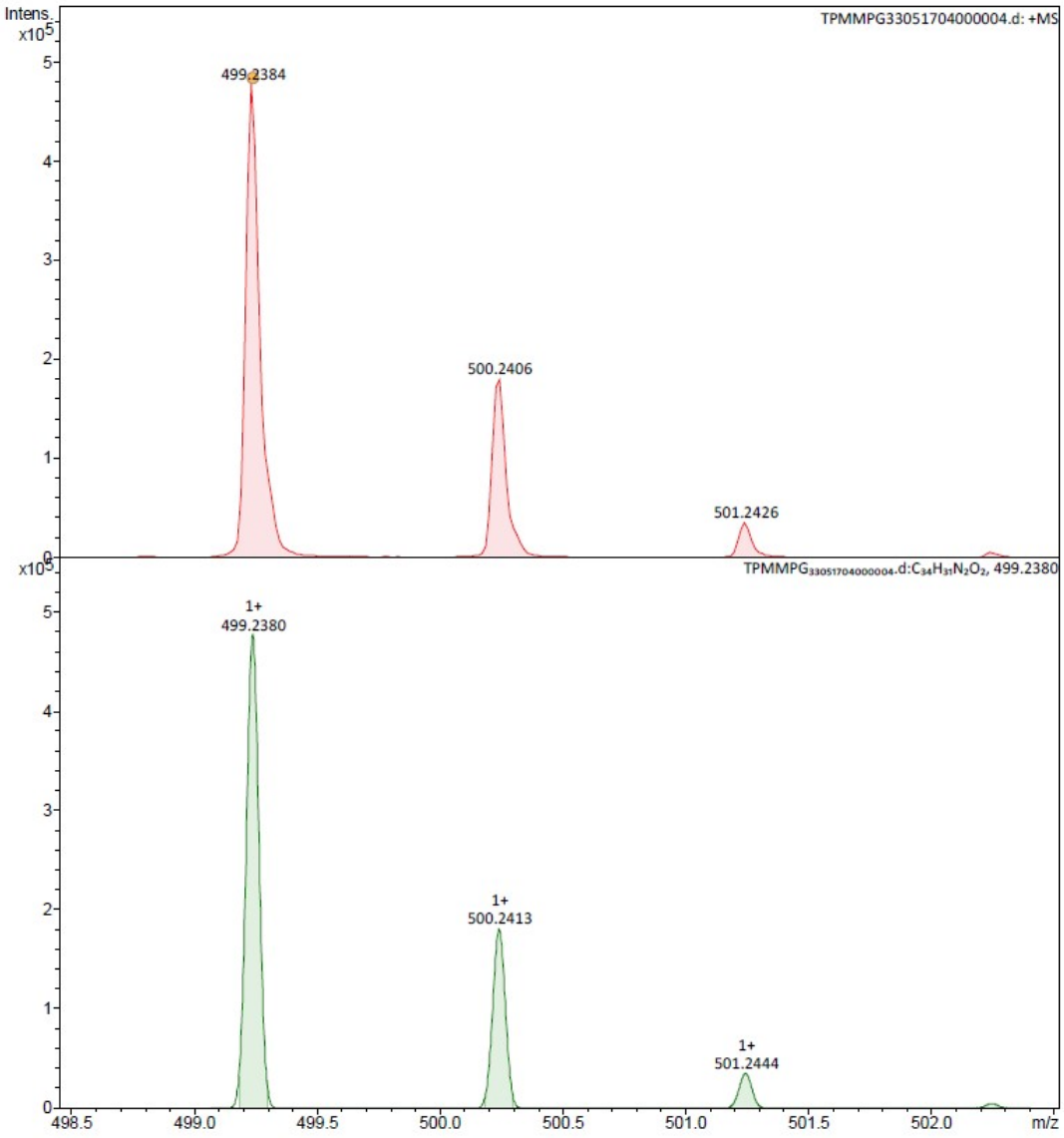

Figure S6. High resolution mass spectrum of **N,N'PhC$_3$Ind**.

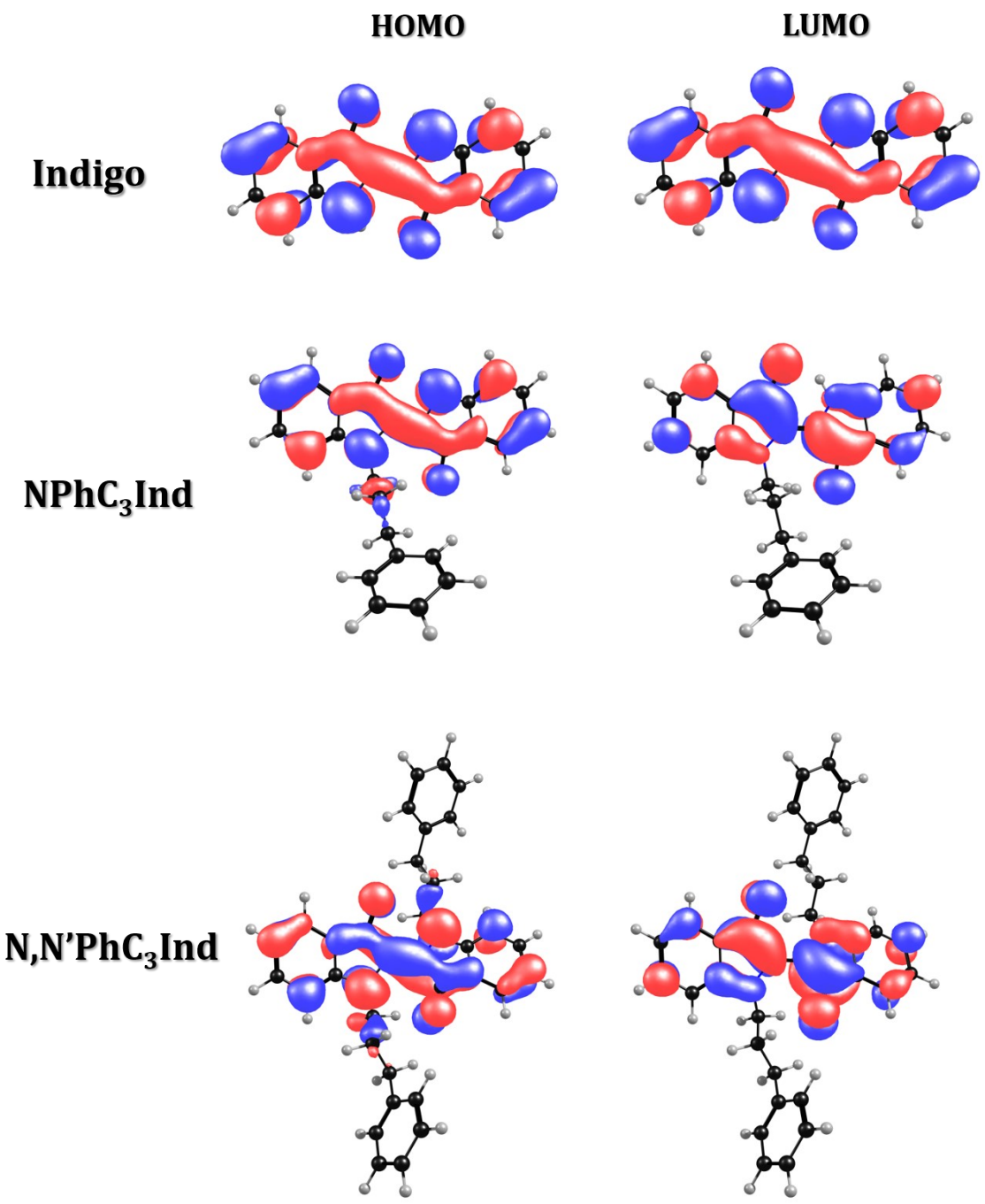

Figure S7. Orbital contours of the HOMO and LUMO for the indigo (**IND**), **NPhC$_3$Ind** and **N,N'PhC$_3$Ind** in DMF.

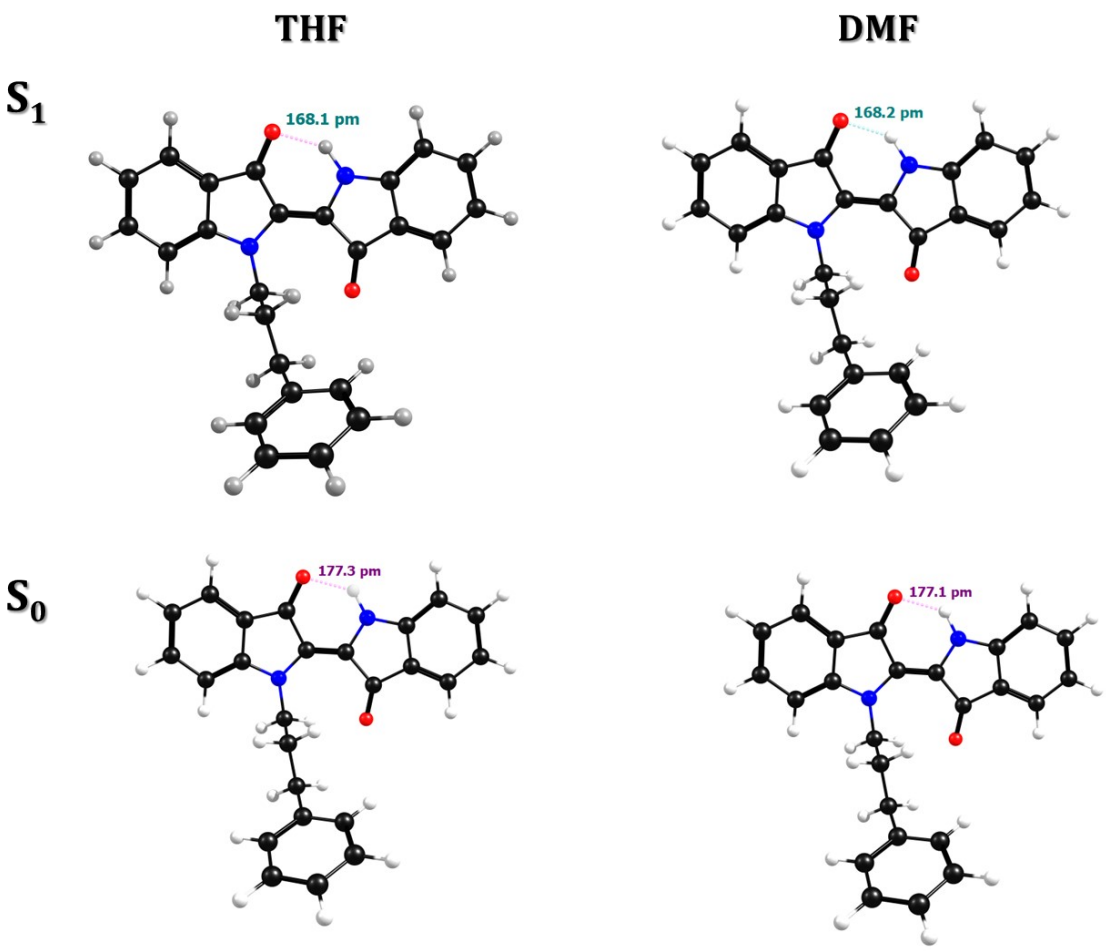

Figure S8. Optimized structures in the S_0 and S_1 electronic states for the **NPhC$_3$Ind** in THF and DMF. The bond distance between the oxygen in C=O and the hydrogen in N-H decreases from 177.3 pm in S_0 to 168.1 pm in S_1 in THF and 177.1 pm in S_0 to 168.2 pm in S_1 in DMF, thus facilitating enol formation.

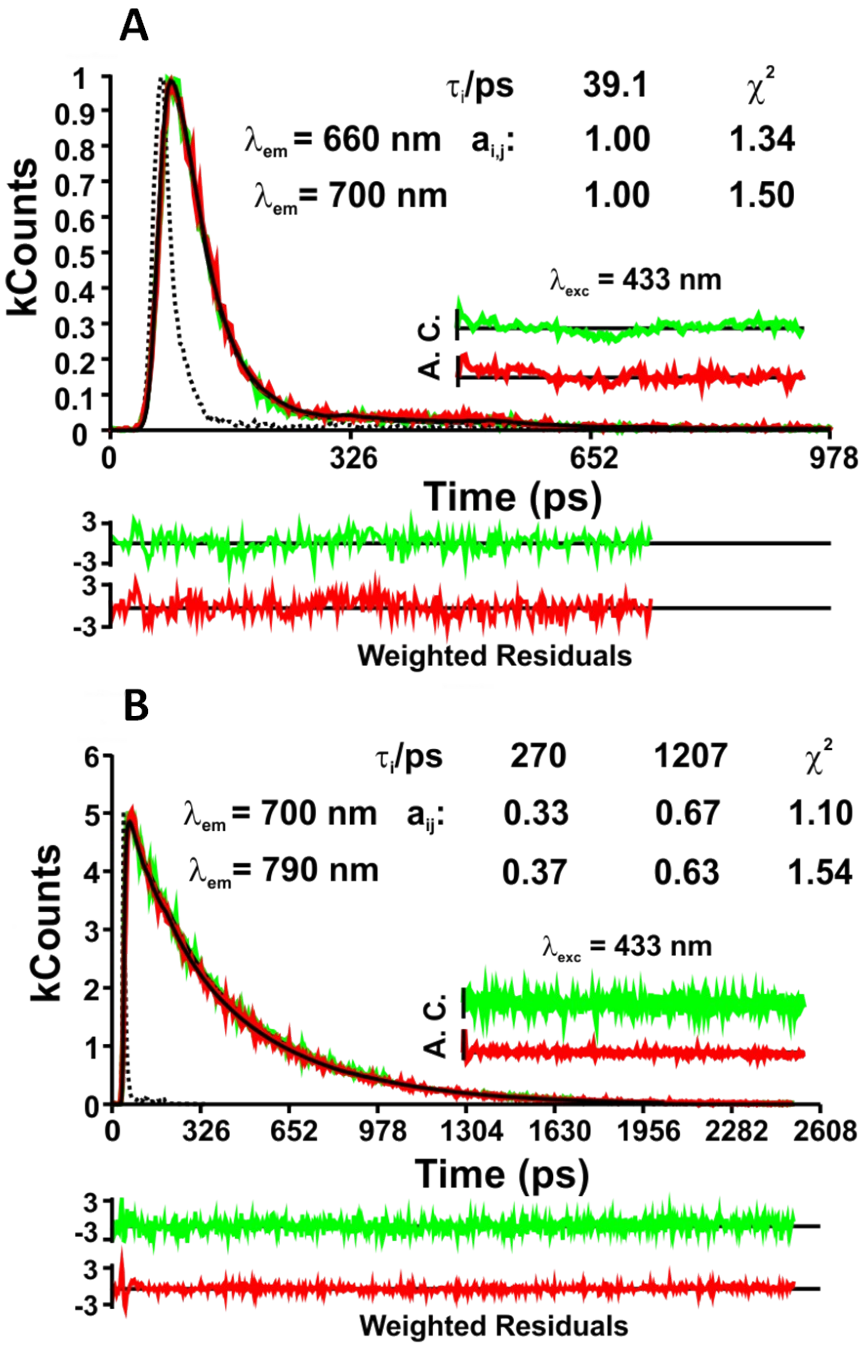

Figure S9. Fluorescence decay and pulse instrumental response obtained for (A) **NPhC$_3$Ind** and (B) **N,N'PhC$_3$Ind** in MCH at T = 293 K. The emission wavelengths and obtained decays times are shown as insets in the figure. For better judgment of the quality of the fits, the weighed residuals (WRs), autocorrelation functions (ACs), and chi-squared (χ^2) values are also shown.

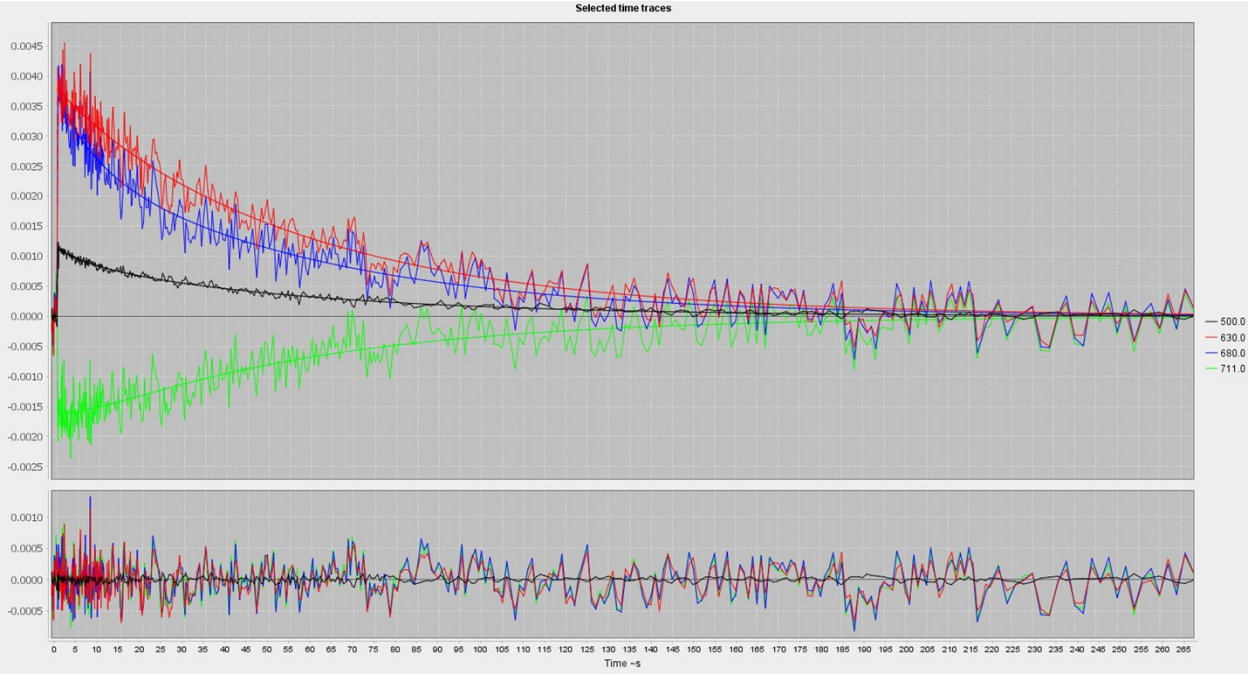

the investigated **NPhC$_3$IND** in 2MeTHF solution. Also presented, for the judgment of the quality of the fits, are the weighted residuals distribution (W.R.).

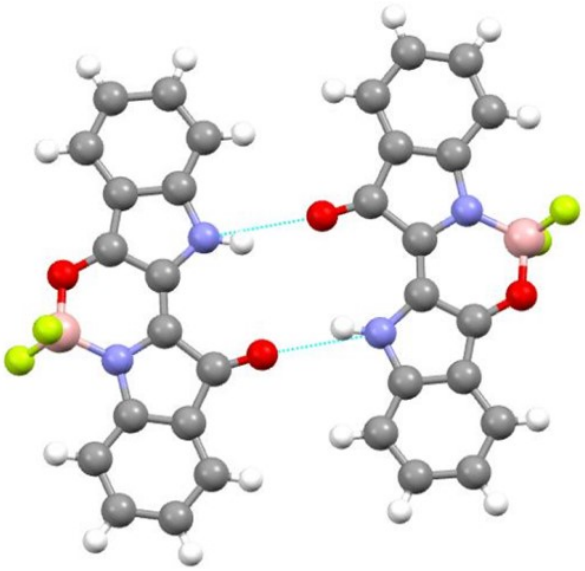

Figure S11. Dimeric structure observed in single-crystal X-ray data of a mono-substituted indigo, a BF_3-complexed indigo derivative.[8]

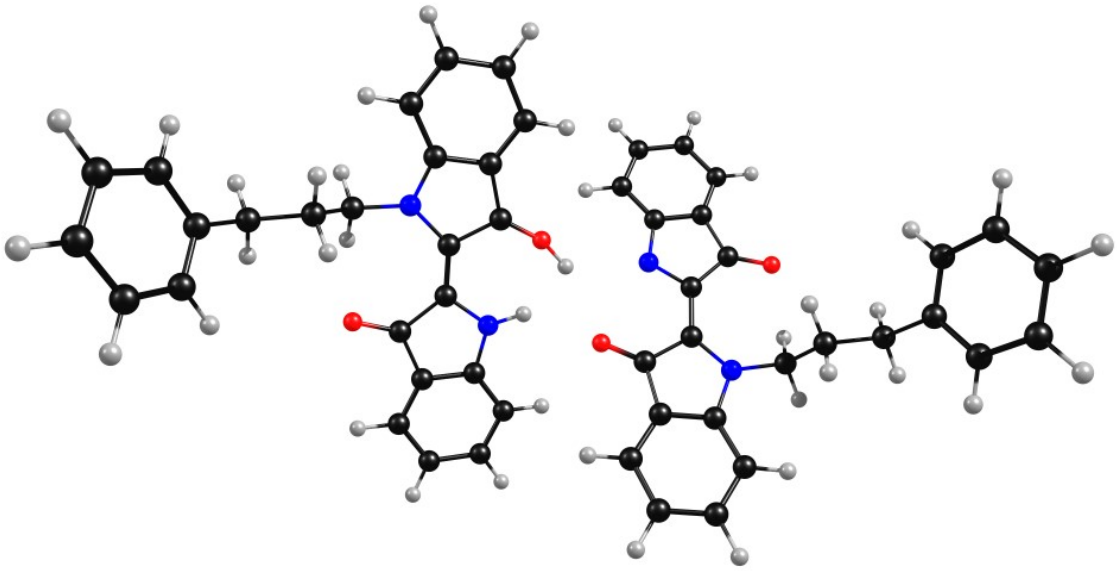

Figure S12. A^-/AH^+ acid/base conjugated pair for **NPhC$_3$Ind** in MCH.

References

1. J. S. Seixas de Melo, R. Rondão, H. D. Burrows, M. J. Melo, S. Navaratnam, R. Edge and G. Voss, *ChemPhysChem*, 2006, **7**, 2303-2311.
2. S. L. Murov, I. Carmichael and G. L. Hug, *Handbook of photochemistry*, Crc Press, 1993.
3. M. W. Schmidt, K. K. Baldridge, J. A. Boatz, S. T. Elbert, M. S. Gordon, J. H. Jensen, S. Koseki, N. Matsunaga, K. A. Nguyen and S. Su, *Journal of computational chemistry*, 1993, **14**, 1347-1363.
4. J. Pina, J. Seixas de Melo, H. Burrows, A. Maçanita, F. Galbrecht, T. Bunnagel and U. Scherf, *Macromolecules*, 2009, **42**, 1710-1719.
5. G. Striker, V. Subramaniam, C. A. Seidel and A. Volkmer, *The Journal of Physical Chemistry B*, 1999, **103**, 8612-8617.
6. J. J. Snellenburg, S. Laptenok, R. Seger, K. M. Mullen and I. H. van Stokkum, *Journal of Statistical Software*, 2012, **49**, 1-22.
7. D. C. Nobre, E. Delgado-Pinar, C. Cunha, A. M. Galvão and J. S. Seixas de Melo, *Dyes and Pigments*, 2023, **212**, 111116.
8. S. Wang, Y. Zhao, C. Zhao, L. Liu and S. Yu, *J. Fluor. Chem.*, 2013, **156**, 236-239.